View metadata, citation and similar papers at core.ac.uk

brought to you by CORE

東北大学機関リポジトリ
TOUR
Tohoku University Repository

Momentum-dependent charge excitations of a two-leg ladder: Resonant inelastic x-ray scattering of (La,Sr,Ca)14Cu24041

著者	小池　洋二
journal or publication title	Physical review. B
volume	76
number	4
page range	045124-1-045124-7
year	2007
URL	http://hdl.handle.net/10097/34911

Momentum-dependent charge excitations of a two-leg ladder: Resonant inelastic x-ray scattering of $(La,Sr,Ca)_{14}Cu_{24}O_{41}$

K. Ishii,[1,*] K. Tsutsui,[2] T. Tohyama,[3] T. Inami,[1] J. Mizuki,[1] Y. Murakami,[1,4] Y. Endoh,[1,5] S. Maekawa,[2] K. Kudo,[2,6] Y. Koike,[6] and K. Kumagai[7]

[1]*Synchrotron Radiation Research Unit, Japan Atomic Energy Agency, Hyogo 679-5148, Japan*

[2]*Institute for Materials Research, Tohoku University, Sendai 980-8577, Japan*

[3]*Yukawa Institute for Theoretical Physics, Kyoto University, Kyoto 606-8502, Japan*

[4]*Department of Physics, Graduate School of Science, Tohoku University, Sendai 980-9578, Japan*

[5]*International Institute for Advanced Studies, Kizu, Kyoto 619-0025, Japan*

[6]*Department of Applied Physics, Graduate School of Engineering, Tohoku University, Sendai 980-8579, Japan*

[7]*Division of Physics, Graduate School of Science, Hokkaido University, Sapporo 060-0810, Japan*

(Received 2 February 2007; revised manuscript received 6 May 2007; published 31 July 2007)

Momentum-dependent charge excitations of a two-leg ladder are investigated by resonant inelastic x-ray scattering of $(La,Sr,Ca)_{14}Cu_{24}O_{41}$. In contrast to the case of a square lattice, momentum dependence of the Mott gap excitation of the ladder exhibits little change upon hole doping, indicating the formation of hole pairs. Theoretical calculation based on a Hubbard model qualitatively explains this feature. In addition, experimental data show an intraband excitation as continuum intensity below the Mott gap and it appears at all the momentum transfers simultaneously. The intensity of the intraband excitation is proportional to the hole concentration of the ladder, which is consistent with optical conductivity measurements.

DOI: 10.1103/PhysRevB.76.045124 PACS number(s): 74.25.Jb, 74.72.Jt, 78.70.Ck

I. INTRODUCTION

Physics in low-dimensional antiferromagnetic spin systems has attracted great interest in connection with high-T_c superconductivity. A two-dimensional $S=1/2$ square lattice, which is a common structure for high-T_c superconductors, shows an antiferromagnetic order, while strong quantum fluctuation suppresses long-range order in a one-dimensional chain. An antiferromagnetic $S=1/2$ two-leg ladder lies between the chain and the square lattice from a structural point of view. It surprisingly shows a different magnetic ground state from the one- and two-dimensional cases, namely, a spin singlet state with a finite energy gap.[1] Furthermore, it is predicted that holes introduced into the two-leg ladder tend to form binding pairs through the rung, which might condense into superconductivity. A representative material system with the hole-doped two-leg ladder is $A_{14}Cu_{24}O_{41}$ (A =La, Y, Sr, and Ca), and Uehara *et al.* actually demonstrated superconductivity in $Sr_{0.4}Ca_{13.6}Cu_{24}O_{41.84}$ under high pressure.[2]

An important feature of the superconductivity in $Sr_{14-x}Ca_xCu_{24}O_{41}$ is that it occurs by carrier doping in the low-dimensional antiferromagnetic spin system. This feature is common to the CuO_2 plane. Therefore, the evolution of the electronic structure upon hole doping is one of the key issues for understanding superconductivity. Furthermore, recent resonant soft x-ray scattering studies demonstrated that $Sr_{14-x}Ca_xCu_{24}O_{41}$ has a quantum state competing to superconductivity at ambient pressure, namely, doped holes form a Wigner crystal in the ladder.[3,4] Differences in the electronic structure of the hole-doped states of the two-leg ladder and of the square lattice are expected, and they should be clarified in detail. In this respect, resonant inelastic x-ray scattering (RIXS), which has been developed recently by utilizing brilliant synchrotron radiation x rays, is a suitable experimental tool. It can measure charge dynamics with momentum resolution, and the electronic excitations related to the Cu orbital are resonantly enhanced by tuning the incident photon energy to the Cu K edge. RIXS has been applied so far to some high-T_c superconductors and their parent Mott insulators to measure the interband excitation across the Mott gap and the intraband excitation below the gap.[5–12]

In this paper, we report on RIXS study of $(La,Sr,Ca)_{14}Cu_{24}O_{41}$, focusing on the electronic excitations in the ladder. We find that the interband excitation across the Mott gap has characteristic dispersion along the leg and the rung and is insensitive to hole doping, indicating that two holes form a bound state through the rung. The obtained momentum-dependent RIXS spectra are qualitatively reproduced by a theoretical calculation. We also find that the intraband excitation appears at all momenta simultaneously and its intensity is proportional to the hole concentration of the ladder.

$(La,Sr,Ca)_{14}Cu_{24}O_{41}$ is a composite crystal in which a two-leg ladder and an edge-sharing chain coexist with different periodicity. In the parent $Sr_{14}Cu_{24}O_{41}$, the nominal valence of Cu is +2.25 and holes are predominantly in the chain sites. Substitution of Ca for Sr brings about a transfer of the holes from the chain to the ladder.[13,14] On the other hand, holes decrease in both chain and ladder sites when the concentration of trivalent La increases. We select three representative compositions; parent $Sr_{14}Cu_{24}O_{41}$, $La_5Sr_9Cu_{24}O_{41}$, and $Sr_{2.5}Ca_{11.5}Cu_{24}O_{41}$. Hole concentration of $La_5Sr_9Cu_{24}O_{41}$ is very small in both ladder and chain, while $Sr_{2.5}Ca_{11.5}Cu_{24}O_{41}$ has enough holes in the ladder to become a superconductor under high pressure.[15] In order to distinguish excitations of the ladder from those of the chain, we also measured RIXS spectra of $Ca_{2+x}Y_{2-x}Cu_5O_{10}$ which only contains edge-sharing chains.[16]

This paper is organized as follows. After the description of the experimental procedures in Sec. II, we first present

 ©2007 The American Physical Society

incident energy dependence of the parent $Sr_{14}Cu_{24}O_{41}$ in Sec. III A. Then, we show in Sec. III B that the excitation observed at 2–4 eV in the RIXS spectra originates from the ladder. Momentum and doping dependence of the interband excitation across the Mott gap and of the intraband excitation below the gap are presented in Secs. III C and III D, respectively. The interband excitation is compared with a theoretical calculation. Finally, we summarize our work in Sec. IV.

II. EXPERIMENTAL DETAILS

RIXS experiments were performed at BL11XU of SPring-8, where a spectrometer for inelastic x-ray scattering is installed.[17] Incident x rays from a SPring-8 standard undulator were monochromatized by a Si (111) double crystal monochromator and a Si (400) channel-cut monochromator. Horizontally scattered x rays were analyzed in energy by a spherically bent Ge (733) analyzer. Total energy resolution estimated from the full width at half maximum of the elastic scattering is about 400 meV. We use Miller indices based on a face centered orthorhombic unit cell of the ladder part to denote absolute momentum transfer. The a and c axes are parallel to the rung and the leg, respectively, and the lattice parameters are $a=11.462$ Å, $b=13.376$ Å, and $c_{\mathrm{ladder}}=3.931$ Å for $Sr_{14}Cu_{24}O_{41}$.[18] The unit lattice vector of the chain is $c_{\mathrm{chain}} \simeq 0.7 c_{\mathrm{ladder}}$.

Single crystals of $(La,Sr,Ca)_{14}Cu_{24}O_{41}$ (Ref. 19) and $Ca_{2+x}Y_{2-x}Cu_5O_{10}$ (Ref. 16) were grown by the traveling-solvent floating-zone method. The surface normal to the stacking direction (b axis) was irradiated by x rays. They were mounted so that the bc plane was parallel to the scattering plane when the a^* component of the momentum transfer was zero. Because the momentum dependence along the b axis is expected to be very small, we selected the b^* component of the momentum transfer where the scattering angle (2θ) was close to 90°; namely, where the momentum transfer is $\vec{Q}=(H,13.5,L)$ for $Sr_{14}Cu_{24}O_{41}$ and $La_5Sr_9Cu_{24}O_{41}$ and $\vec{Q}=(H,12.8,L)$ for $Sr_{2.5}Ca_{11.5}Cu_{24}O_{41}$. It enabled us to reduce the elastic scattering significantly by the polarization factor of the Thomson scattering.[9] All the spectra were measured at room temperature.

III. RESULTS AND DISCUSSION

A. Incident energy dependence

In Fig. 1(a), we plot the incident energy (E_i) dependence of the RIXS spectra of $Sr_{14}Cu_{24}O_{41}$ near the Cu K edge. The momentum transfer here is fixed at $\vec{Q}=(0,13.5,0)$, which corresponds to the Brillouin zone center of the ladder and the chain. Excitation at 2–4 eV is resonantly enhanced near 8984 and 8993 eV. Figure 1(b) shows the x-ray absorption spectra (XAS) of $Sr_{14}Cu_{24}O_{41}$. The spectra were measured by the total fluorescence yield method. The photon polarization ($\vec{\varepsilon}$) in the spectrum of $\vec{\varepsilon}\|\vec{b}$ is perpendicular to the ladder plane and the Cu-O plaquettes of the chain. On the other hand, the polarization is parallel to them in $\vec{\varepsilon}\|\vec{c}$. Each spectrum has two peaks. By analogy with the CuO_2 plane,[20] we can assign the peaks at lower energies (8985 and 8995 eV)

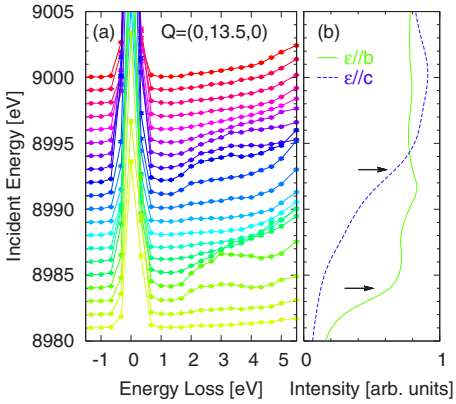

FIG. 1. (Color online) (a) Incident energy dependence of RIXS spectra of $Sr_{14}Cu_{24}O_{41}$. The incident energy for each scan can be read from the vertical axis. (b) Fluorescence spectra of $\vec{\varepsilon}\|\vec{b}$ (solid line) and $\vec{\varepsilon}\|\vec{c}$ (broken line). The arrows indicate incident energies where inelastic scattering at 2–4 eV is resonantly enhanced.

and higher energies (8992 and 9000 eV) to the well-screened ($1\underline{s}3d^{10}\underline{L}4p$) and poorly screened ($1\underline{s}3d^9 4p$) core hole final states, respectively, where $\underline{L}$ denotes the hole in a ligand oxygen.

In general, a resonant energy of inelastic scattering is close to a peak in the absorption spectrum because the final state of XAS corresponds to an intermediate state of RIXS process. The polarization of the incident photon ($\vec{\varepsilon}_i$) is almost parallel to $\hat{b}+\hat{c}$ at $\vec{Q}=(0,13.5,0)$, where $\hat{b}$ and $\hat{c}$ are the unit vectors along the b and c axes, respectively. Therefore, the $\hat{c}$ component in $\vec{\varepsilon}_i$ is responsible for the resonance at 8984 eV, while the $\hat{b}$ component in $\vec{\varepsilon}_i$ contributes at 8993 eV. In other words, the resonant enhancement of inelastic scattering occurs slightly below the well-screened states in $Sr_{14}Cu_{24}O_{41}$. Incident photon energy is fixed at either 8984 eV or 8993 eV in the following spectra.

B. Assignment of 2–4 eV excitation

In order to distinguish excitations of the ladder from those of the chain, we compared RIXS spectra of $Sr_{14}Cu_{24}O_{41}$ to those of $Ca_2Y_2Cu_5O_{10}$ which only contains edge-sharing chains. The crystal structures of $(La,Sr,Ca)_{14}Cu_{24}O_{41}$ and $Ca_{2+x}Y_{2-x}Cu_5O_{10}$ are presented in Figs. 2(a) and 2(b), respectively. In $(La,Sr,Ca)_{14}Cu_{24}O_{41}$, the ladder layers and the edge-sharing chain layers are stacked alternatively along the b axis, and the cations are inserted between the layers. On the other hand, $Ca_{2+x}Y_{2-x}Cu_5O_{10}$ contains only edge-sharing chain layers.[21] In this sense, $Ca_{2+x}Y_{2-x}Cu_5O_{10}$ is a suitable material of edge-sharing chain to compare with $(La,Sr,Ca)_{14}Cu_{24}O_{41}$.

In Fig. 2(c), we show the RIXS spectra of $Sr_{14}Cu_{24}O_{41}$ and $Ca_2Y_2Cu_5O_{10}$. Both spectra were measured at the Brillouin zone center of the chain and the ladder and at the same incident photon energy $E_i=8993$ eV. Polarization of the incident photon is also the same, as shown by the arrows in Figs. 2(a) and 2(b). The excitation at 2–4 eV is almost absent in $Ca_2Y_2Cu_5O_{10}$ except for a very weak peak at 2 eV,

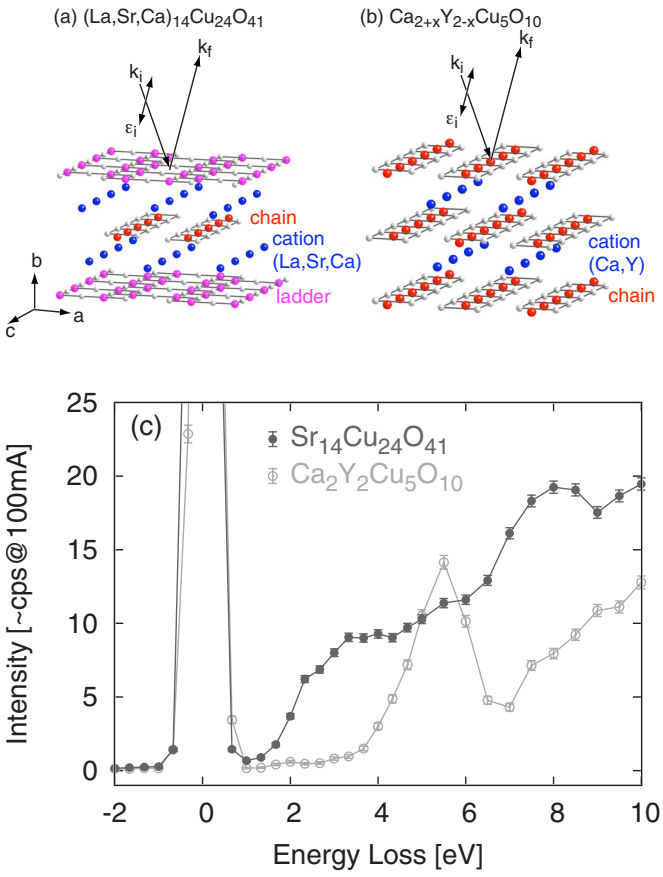

FIG. 2. (Color online) Crystal structure of (a) $(La,Sr,Ca)_{14}Cu_{24}O_{41}$ and (b) $Ca_{2+x}Y_{2-x}Cu_5O_{10}$. (c) RIXS spectra of $Sr_{14}Cu_{24}O_{41}$ and $Ca_2Y_2Cu_5O_{10}$. The experimental configurations of these spectra are shown by arrows in (a) and (b). Here, k_i and k_f are the wave vectors of incident and the scattered photons, respectively, and ε_i is the polarization of the incident photon.

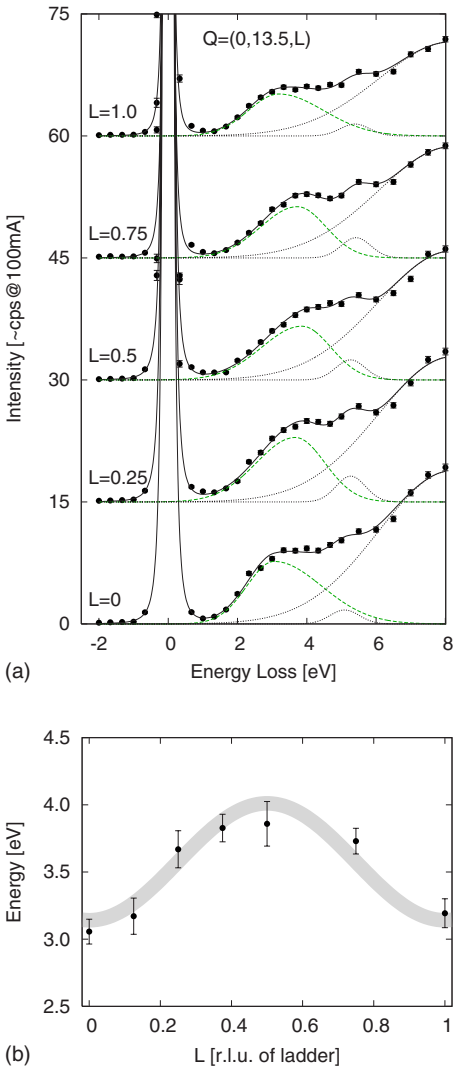

FIG. 3. (Color online) (a) RIXS spectra of $Sr_{14}Cu_{24}O_{41}$ at $\vec{Q}=(0,13.5,L)$ $(0\leqslant L\leqslant 1)$. Filled circles are experimental data and the lines are results of fitting described in the text. Solid lines are the overall spectral shape which is the sum of elastic line, Mott gap excitation (dashed lines), and the excitations at 5 and 8 eV (dotted lines). (b) Dispersion relation of the 2–4 eV excitation. Solid thick line is a guide to the eyes. The peak position is folded at $L=0.5$ which corresponds to the Brillouin zone boundary of the ladder.

while it has a large intensity in $Sr_{14}Cu_{24}O_{41}$. This is clear evidence that the RIXS intensity at 2–4 eV in $Sr_{14}Cu_{24}O_{41}$ comes from the ladder. In $Ca_{2+x}Y_{2-x}Cu_5O_{10}$, we can introduce holes in the chain by substituting Ca for Y (x). All the Cu atoms are divalent at $x=0$. It is notable that RIXS spectra of $Ca_{2+x}Y_{2-x}Cu_5O_{10}$ are almost independent of x. Detailed results regarding $Ca_{2+x}Y_{2-x}Cu_5O_{10}$ will be published elsewhere. At a higher energy region, the RIXS spectra of $Ca_{2+x}Y_{2-x}Cu_5O_{10}$ are similar to those of another cuprate composing edge-sharing chains, Li_2CuO_2;[22] that is, peak features are observed near 5.5 and 8 eV.

Another piece of evidence is the momentum dependence which was measured across a Brillouin zone boundary. Figure 3(a) shows RIXS spectra of $Sr_{14}Cu_{24}O_{41}$ at $\vec{Q}=(0,13.5,L)$ $(0\leqslant L\leqslant 1)$. Incident photon energy (E_i) is 8993 eV. In order to elucidate the dispersion relation qualitatively, we analyzed the observed data by fitting. The tail of the elastic scattering or quasielastic component on the energy loss side was evaluated from the energy gain side. We approximated the excitation at 2–4 eV by an asymmetric Gauss function. Four parameters, peak height, peak position, and two peak widths are variable from spectrum to spectrum. Different values are used for the width above and below the energy of the peak position. When a symmetric Gauss function was used, we obtained qualitatively similar results. In addition, the excitations 5 and 8 eV were included as Gauss functions. This fitting analysis well reproduces the spectral shape at all the momenta, as shown by the solid lines in Fig. 3(a). The obtained peak positions of the 2–4 eV excitation are plotted as a function of momentum transfer along the leg direction in Fig. 3(b). The Brillouin zone boundary of the ladder is $L=0.5$ while that of the chain is $L\simeq 0.7$. It is clear that the spectra are folded at $L=0.5$, and this result also confirms that the excitation at 2–4 eV comes from the ladder. Furthermore, in accordance with optical conductivity measurement,[14,23] we attribute it to the excitation across the Mott gap, more precisely from the Zhang-Rice band to the upper Hubbard band, of the ladder.

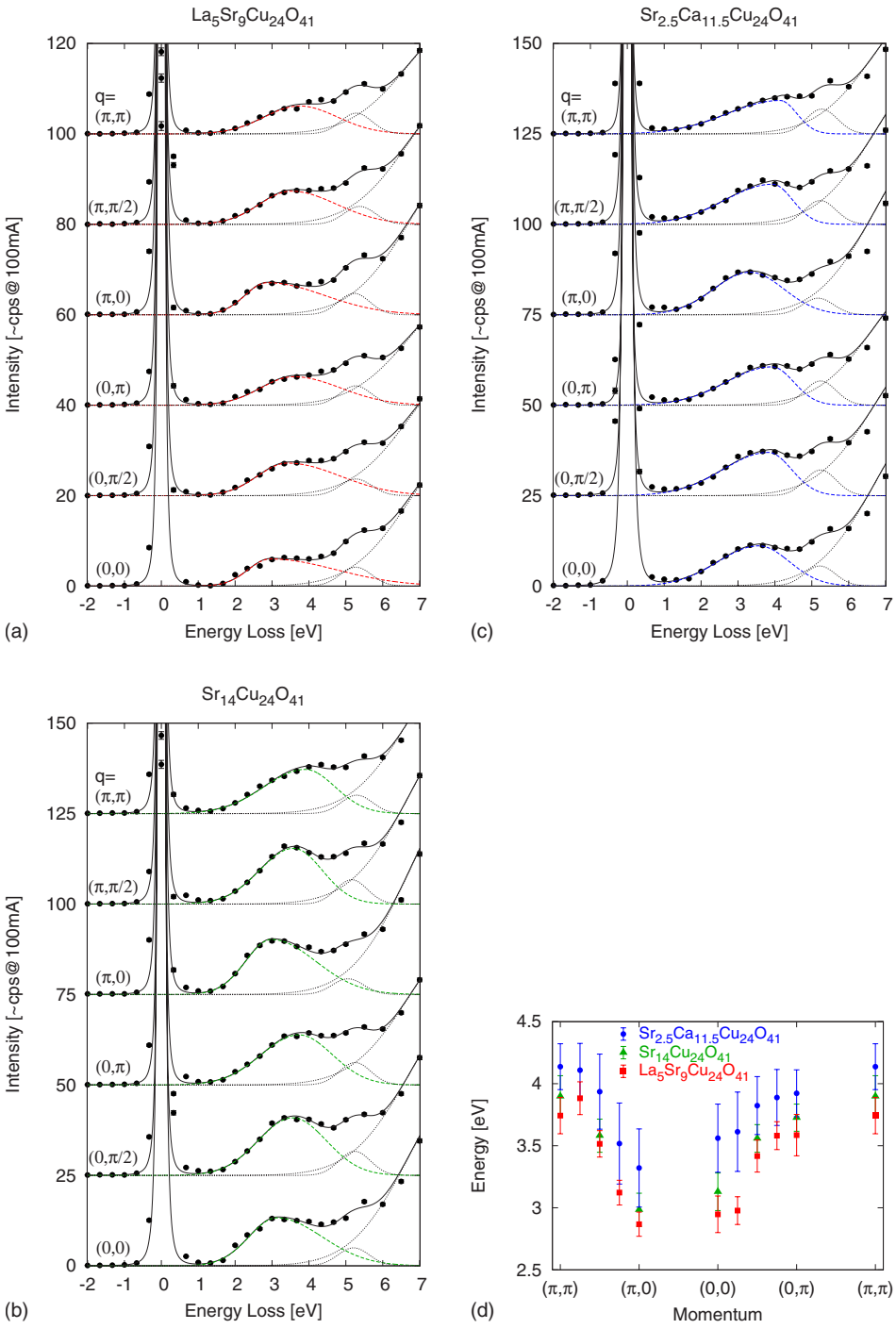

FIG. 4. (Color online) RIXS spectra of (a) $La_5Sr_9Cu_{24}O_{41}$, (b) $Sr_{14}Cu_{24}O_{41}$, and (c) $Sr_{2.5}Ca_{11.5}Cu_{24}O_{41}$. Filled circles are experimental data and the lines are results of fitting. Solid lines are the overall spectral shape which is the sum of elastic line, Mott gap excitation (dashed lines), and the excitations at 5 and 8 eV (dotted lines). (d) Dispersion relation of the Mott gap excitation.

C. Interband excitation

We discuss the momentum and doping dependence of the Mott gap excitation in this section. Figure 4 shows the momentum dependence of the spectra of (a) $La_5Sr_9Cu_{24}O_{41}$, (b) $Sr_{14}Cu_{24}O_{41}$, and (c) $Sr_{2.5}Ca_{11.5}Cu_{24}O_{41}$. These spectra were measured at E_i=8984 eV. Hole concentration in the ladder is smallest in $La_5Sr_9Cu_{24}O_{41}$, while it is largest in $Sr_{2.5}Ca_{11.5}Cu_{24}O_{41}$. Here, we consider momentum transfer along the rung direction in addition to the leg one. The reduced momentum transfer $\vec{q}$ is represented as $\vec{q}=(q_{\mathrm{rung}},q_{\mathrm{leg}})$ and q_{rung} is either 0 or π. We performed the same fitting analysis as in the previous section and the obtained dispersion relations are summarized in Fig. 4(d). The Mott gap excitation seen at 2–4 eV shifts to higher energy with q_{leg}. When the spectra are compared along the rung direction, the spectral weights of the Mott gap excitation of $\vec{q}=(\pi,\pi)$ are located at a slightly higher energy region than those of $\vec{q}=(0,\pi)$. We emphasize that these features of the momentum dependence are similar in the three compounds, even though peak positions shift to higher energy with increasing the hole concentration in the ladder, probably due to the shift of Fermi energy.

The effect of hole doping on the dispersion relation of the ladder is smaller than that of the two-dimensional square

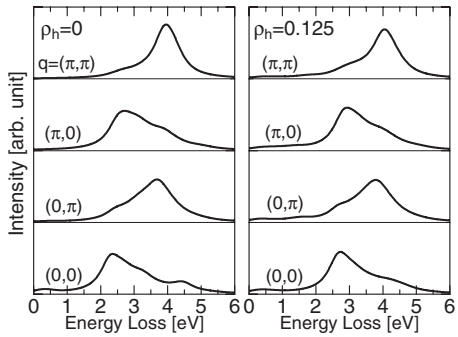

FIG. 5. The RIXS spectra of undoped ($\rho_h=0$, left panel) and hole-doped ($\rho_h=2/16=0.125$, right panel) 2×8 Hubbard ladder models. The model parameters are $U/t=10$, $U_c/t=15$, $\Gamma/t=1$, with $t=0.35$ eV. The δ functions are convoluted with a Lorentzian broadening of t.

lattice. In $La_{2-x}Sr_xCuO_4$ ($x=0.17$),[7] the dispersion of the onset energy of the Mott gap excitation becomes smaller than that in the undoped case, which is related to the reduction of the antiferromagnetic spin correlation by the hole doping.[24] Note that the present RIXS spectra of the ladder along the leg direction are also different from that of the corner-sharing chain system in which the RIXS intensity accumulates in a narrow energy region at the Brillouin zone boundary.[8,25,26]

In order to confirm the characteristics of the ladder theoretically, we carried out the calculation of the RIXS spectrum by using the numerically exact diagonalization technique on small clusters. Mapping the Zhang-Rice band onto the lower Hubbard one,[27] we employ a single-band Hubbard ladder model. The model includes the hopping term of the electrons (t) and the on-site Coulomb interaction term (U). The RIXS spectrum is expressed as a second-order process of the dipole transition between Cu $1s$ and $4p$ orbitals, where a Coulomb interaction between the $1s$ core and the $3d$ electron, U_c, is explicitly included.[28] The values of the model parameters are set to be $U/t=10$, $U_c/t=15$, with $t=0.35$ eV. The inverse of the lifetime of the intermediate state is assumed to be $\Gamma/t=1$.

Figure 5 shows the calculated RIXS spectra for undoped (left panel) and hole-doped (right panel) cases, where the hole concentration is $\rho_h=2/16=0.125$ in the latter case. We find characteristic features in the spectra which are similar to the observed ones. The peak position of the spectrum at $q_{\mathrm{leg}}=\pi$ is located at a higher energy than that at $q_{\mathrm{leg}}=0$ for each q_{rung}. Furthermore, the spectral weight at $\vec{q}=(\pi,\pi)$ is higher in energy than that at $\vec{q}=(0,\pi)$. The feature that the energy position at (π,π) is higher than that at $(0,\pi)$ is similar to that of the undoped two-dimensional square-lattice case.[28] On the other hand, the doping dependence of RIXS spectra is different from that of the square lattice. While the momentum dependence of the RIXS for the Mott gap excitation changes in the square lattice upon doping,[24] it does not change in the ladder. In addition, the spectral weight shifts to a higher energy after hole doping, which is also consistent with the experimental results. Thus, we conclude that the effect of hole doping seen in Fig. 4 is characteristic of the ladder.

In the square-lattice system, momentum dependence of the Mott gap excitation spectrum is significantly influenced by the antiferromagnetic spin correlations. The spectrum becomes broad and has a weak dispersion upon hole doping, reflecting the decreasing of the antiferromagnetic spin correlation.[24] On the other hand, it is established by various experiments, such as inelastic neutron scattering,[29] NMR,[30–32] and thermal conductivity,[19] that the spin gap of the ladder robustly persists irrespective of the hole concentration. The holes introduced into the ladder can be paired so as not to destroy the local singlet states along rungs in the undoped Cu sites. Since the Mott gap excitation occurs at undoped Cu sites, our RIXS result that the excitation in the ladder is insensitive to the hole doping can be understood in the scheme of the hole pair formation. Both the results of the CuO_2 plane and the ladder show that the hole-doping effect on the Mott gap excitation is related to the underlying magnetic states, that is, spectral shape in $La_{2-x}Sr_xCuO_4$ changes upon hole doping associated with the reduction of the antiferromagnetic correlation, while the Mott gap excitation of the ladder is unchanged as the spin gap state is.

Based on a resistivity measurement under high pressure, it has been proposed that holes confined in a ladder begin to move along the rung direction beyond the ladder and the spin gap collapses when superconductivity occurs.[33,34] Since x rays at the Cu K edge pass through a pressure cell, such pressure-induced dimensional crossover may be detectable by RIXS in the future.

D. Intraband excitation

Next, we discuss the intraband excitation in the ladder. In doped Mott insulators, two kinds of excitations appear in the RIXS spectra. One is an interband excitation across the Mott gap. This excitation is observed at 2–4 eV in $(La,Sr,Ca)_{14}Cu_{24}O_{41}$, and its dispersion relation is independent of the hole concentration of the ladder, as discussed in the previous section. The other excitation appears as continuum intensity below the Mott gap energy (~2 eV) when holes are doped. This excitation is related to the dynamics of the doped holes in the Zhang-Rice band and we call it intraband excitation. In Fig. 6(a), we replot the RIXS spectra in Figs. 4(a)–4(c), where the spectra are normalized to the intensity at 2–4 eV. Normalization factors are 1.8, 1.0, and 0.85 for $La_5Sr_9Cu_{24}O_{41}$, $Sr_{14}Cu_{24}O_{41}$, and $Sr_{2.5}Ca_{11.5}Cu_{24}O_{41}$, respectively, and the intensities multiplied by these values are presented in Fig. 6(a). The normalization factors are common for all the momenta. The intraband excitation in the ladder exhibits weak momentum dependence and appears at all momenta simultaneously. The intensity is largest in $Sr_{2.5}Ca_{11.5}Cu_{24}O_{41}$, which is expected judging from the hole concentration in the ladder.

In order to analyze the intraband excitation semiquantitatively, we estimate the intensity of the intraband excitation (I_{intra}) by

$$I_{\mathrm{intra}}=\frac{\sum_{\omega=1.00,1.33\ \mathrm{eV}} I(\omega)-I(-\omega)}{1-\delta}, \qquad (1)$$

where $I(\omega)$ is the RIXS intensity at the energy loss of ω in Fig. 6(a) and δ is the hole number per one Cu atom in the

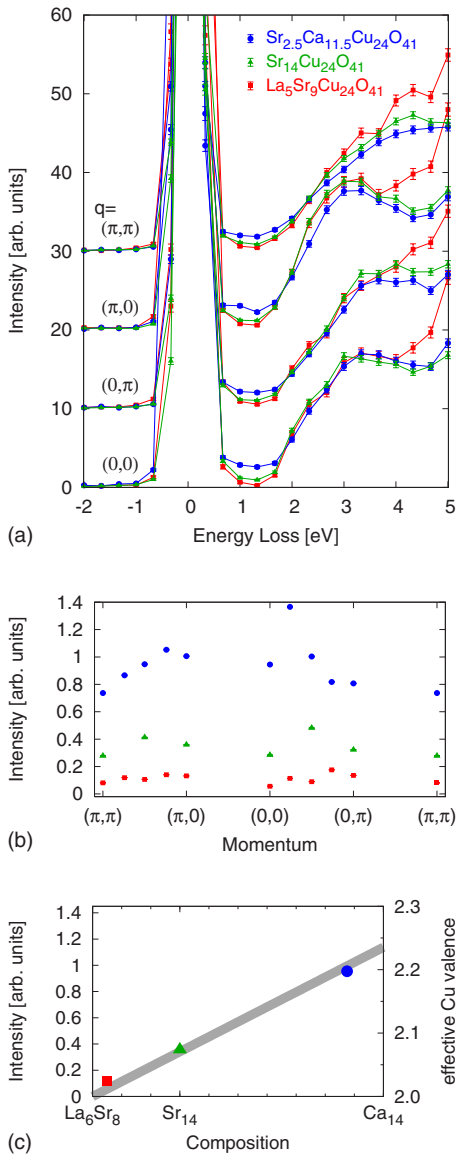

FIG. 6. (Color online) (a) Comparison of the RIXS spectra of $(La,Sr,Ca)_{14}Cu_{24}O_{41}$ which shows the hole-doping dependence. The spectra are normalized to the intensity of the Mott gap excitation at 2–4 eV. (b) Intensity of the intraband excitation as a function of momentum. (c) Momentum-averaged intensity shown in (b) plotted against the composition. The solid line shows the effective valence of Cu in the ladder determined from the optical conductivity in Ref. 14. The symbols in (b) and (c) denote the same composition as those in (a).

ladder. The effective valence of the Cu atom in the ladder is represented as $2+\delta$. Here, we use the term "effective valence" because doped holes predominantly occupy the O $2p$ orbitals in the copper oxides. We subtracted the intensities of $\omega<0$ (anti-Stokes region) to remove the quasielastic component. Assuming that the intensity of the Mott gap excitation at 2–4 eV is proportional to the number of occupied electrons $(1-\delta)$, we divided $I(\omega)$ by $1-\delta$, where the effective Cu valence given in Ref. 14 was used for δ. The obtained I_{intra} is a reasonable estimation of the intensity of the intraband excitation normalized to the intensity of Mott gap excitation in each material. We plot I_{intra} as a function of momentum transfer in Fig. 6(b). The spectral weight of the intraband intensity is rather independent of the momentum transfer, even at a low hole concentration in $Sr_{14}Cu_{24}O_{41}$. In contrast, the doping effect on the intraband excitation in the two-dimensional $La_{2-x}Sr_xCuO_4$ exhibits momentum dependence; that is, a low energy continuum appears at $\vec{q}=(0,0)$ and $(\pi,0)$ at the optimum doping[7] and it extends to (π,π) at the overdoping.[11] We took the average of the intensity for all momenta for each composition and plotted them in Fig. 6(c). We also show the relation between the composition and effective Cu valence of the ladder determined from the optical conductivity which is a probe of the charge dynamics at $q=0$. The RIXS intensity of the intraband excitation is proportional to the effective Cu valence, namely, hole concentration in the ladder, being consistent with the doping dependence of optical conductivity reported previously.[14] This is the first evaluation of the intraband excitation by RIXS as a function of the hole concentration and the fact that the intraband excitation seen in RIXS spectra is proportional to the carrier number is quite reasonable. Our results demonstrate that RIXS has a great potential to reveal the momentum-dependent charge dynamics below the Mott gap, which is important in the physics of doped Mott insulators.

IV. SUMMARY

We have performed a RIXS experiment on $(La,Sr,Ca)_{14}Cu_{24}O_{41}$ to measure the charge dynamics in the two-leg ladder. We found resonantly enhanced excitations at 2–4 eV near the well-screened intermediate states. By distinguishing these from the excitations in the edge-sharing chain, we successfully observed ladder components of both interband excitation across the Mott gap and intraband excitation below the gap. The interband excitation has a characteristic dispersion along the leg and the rung and it is insensitive to hole doping, indicating that two holes form a bound state. These momentum-dependent RIXS spectra can be qualitatively reproduced by a theoretical calculation. On the other hand, the intraband excitation appears at all momenta simultaneously and is proportional to the hole concentration of the ladder. These characteristics of the RIXS demonstrate that the evolution of the electronic structure upon hole doping is different from that of the CuO_2 plane.

ACKNOWLEDGMENTS

This work was performed under the interuniversity cooperative research program of the Institute of Materials Research, Tohoku University and financially supported by the Grant-in-Aid for Scientific Research on Priority Areas "Invention of Anomalous Quantum Materials" from the Ministry of Education, Culture, Sports, Science, and Technology. K.T., T.T., and S.M. were also supported by Next Generation Super Computing Project (Nanoscience Program) of MEXT and CREST. The numerical calculations were carried out at ISSP, University of Tokyo and IMR, Tohoku University.

*kenji@spring8.or.jp

[1] E. Dagotto and T. M. Rice, Science **271**, 618 (1996).
[2] M. Uehara, T. Nagata, J. Akimitsu, H. Takahashi, N. Môri, and K. Kinoshita, J. Phys. Soc. Jpn. **65**, 2764 (1996).
[3] P. Abbamonte *et al.*, Nature (London) **431**, 10789 (2004).
[4] A. Rusydi, P. Abbamonte, H. Eisaki, Y. Fujimaki, G. Blumberg, S. Uchida, and G. A. Sawatzky, Phys. Rev. Lett. **97**, 016403 (2006).
[5] M. Z. Hasan, E. D. Isaacs, Z.-X. Shen, L. L. Miller, K. Tsutsui, T. Tohyama, and S. Maekawa, Science **288**, 1811 (2000).
[6] Y. J. Kim, J. P. Hill, C. A. Burns, S. Wakimoto, R. J. Birgeneau, D. Casa, T. Gog, and C. T. Venkataraman, Phys. Rev. Lett. **89**, 177003 (2002).
[7] Y.-J. Kim, J. P. Hill, S. Komiya, Y. Ando, D. Casa, T. Gog, and C. T. Venkataraman, Phys. Rev. B **70**, 094524 (2004).
[8] K. Ishii *et al.*, Phys. Rev. Lett. **94**, 187002 (2005).
[9] K. Ishii *et al.*, Phys. Rev. Lett. **94**, 207003 (2005).
[10] L. Lu *et al.*, Phys. Rev. Lett. **95**, 217003 (2005).
[11] S. Wakimoto, Y.-J. Kim, H. Kim, H. Zhang, T. Gog, and R. J. Birgeneau, Phys. Rev. B **72**, 224508 (2005).
[12] E. Collart, A. Shukla, J.-P. Rueff, P. Leininger, H. Ishii, I. Jarrige, Y. Q. Cai, S.-W. Cheong, and G. Dhalenne, Phys. Rev. Lett. **96**, 157004 (2006).
[13] M. Kato, K. Shiota, and Y. Koike, Physica C **258**, 284 (1996).
[14] T. Osafune, N. Motoyama, H. Eisaki, and S. Uchida, Phys. Rev. Lett. **78**, 1980 (1997).
[15] K. M. Kojima, N. Motoyama, H. Eisaki, and S. Uchida, J. Electron Spectrosc. Relat. Phenom. **117-118**, 237 (2001).
[16] K. Kudo, S. Kurogi, Y. Koike, T. Nishizaki, and N. Kobayashi, Phys. Rev. B **71**, 104413 (2005).
[17] T. Inami, T. Fukuda, J. Mizuki, H. Nakao, T. Matsumura, Y. Murakami, K. Hirota, and Y. Endoh, Nucl. Instrum. Methods Phys. Res. A **467-468**, 1081 (2001).
[18] E. M. McCarron III, M. A. Subramanian, J. C. Calabrese, and R. L. Harlow, Mater. Res. Bull. **23**, 1355 (1988).
[19] K. Kudo, S. Ishikawa, T. Noji, T. Adachi, Y. Koike, K. Maki, S. Tsuji, and K. Ichi Kumagai, J. Phys. Soc. Jpn. **70**, 437 (2001).
[20] N. Kosugi, Y. Tokura, H. Takagi, and S. Uchida, Phys. Rev. B **41**, 131 (1990).
[21] Y. Miyazaki, I. Gameson, and P. P. Edwards, J. Solid State Chem. **145**, 511 (1999).
[22] Y.-J. Kim, J. P. Hill, F. C. Chou, D. Casa, T. Gog, and C. T. Venkataraman, Phys. Rev. B **69**, 155105 (2004).
[23] Y. Mizuno, T. Tohyama, and S. Maekawa, J. Phys. Soc. Jpn. **66**, 937 (1997).
[24] K. Tsutsui, T. Tohyama, and S. Maekawa, Phys. Rev. Lett. **91**, 117001 (2003).
[25] K. Tsutsui, T. Tohyama, and S. Maekawa, Phys. Rev. B **61**, 7180 (2000).
[26] Y.-J. Kim *et al.*, Phys. Rev. Lett. **92**, 137402 (2004).
[27] F. C. Zhang and T. M. Rice, Phys. Rev. B **37**, 3759 (1988).
[28] K. Tsutsui, T. Tohyama, and S. Maekawa, Phys. Rev. Lett. **83**, 3705 (1999).
[29] S. Katano, T. Nagata, J. Akimitsu, M. Nishi, and K. Kakurai, Phys. Rev. Lett. **82**, 636 (1999).
[30] S. Tsuji, K. Ichi Kumagai, M. Kato, and Y. Koike, J. Phys. Soc. Jpn. **65**, 3474 (1996).
[31] K. I. Kumagai, S. Tsuji, M. Kato, and Y. Koike, Phys. Rev. Lett. **78**, 1992 (1997).
[32] K. Magishi, S. Matsumoto, Y. Kitaoka, K. Ishida, K. Asayama, M. Uehara, T. Nagata, and J. Akimitsu, Phys. Rev. B **57**, 11533 (1998).
[33] T. Nagata *et al.*, Phys. Rev. Lett. **81**, 1090 (1998).
[34] H. Mayaffre, P. Auban-Senzier, M. Nardone, D. Jérome, D. Poilblanc, C. Bourbonnais, U. Ammerahl, G. Dhalenne, and A. Revcolevschi, Science **279**, 345 (1998).